CRYSTAL GROWTH & DESIGN
2007
VOL. 7, NO. 12
2400–2403

Nanocrystalline Titanium to Mesoporous Anatase with High Bioactivity

Ming Wen,[†,‡] Jian-Feng Gu,*[,†] Gang Liu,[‡] Zhen-Bo Wang,[‡] and Jian Lu[#]

School of Materials Science and Engineering, Shanghai Jiao Tong University, Shanghai, 200240, People's Republic of China, Shenyang National Laboratory for Materials Science, Institute of Metals Research, Chinese Academy of Sciences, Shenyang, 110016, People's Republic of China, and Mechanical Engineering Department, The Hong Kong Polytechnic University, Hong Kong, People's Republic of China

Received May 9, 2007; Revised Manuscript Received September 26, 2007

ABSTRACT: In present study, the formation of bioactive anatase on bulk titanium (Ti) by hybrid surface mechanical attrition treatment (SMAT) is reported. A commercial pure Ti plate first underwent SMAT in a vacuum for 1 h to produce a nanocrystalline layer with a thickness of about 30 μm, and then the nanocrystalline Ti (~30 nm) was transformed into mesoporous anatase with a grain size ~10 nm by chemical oxidation and calcination. The mesoporous anatase showed excellent bioactivity while being soaked in simulated body fluid, which could be attributed to the unique nanostructure on the SMAT Ti surface.

Introduction

Commercially pure titanium (Ti) and Ti alloys are the materials of choice in orthopedic and dental applications because of their good biocompatibility, excellent resistance to corrosion, and superior mechanical properties.[1–4] However, due to the limited bioactivity, Ti or Ti alloys are inclined to form fibrous tissue at the Ti−bone interface and thus increase the possibility of implantation loosening over a long period of time.[5,6] On the other hand, calcium phosphate materials and certain glass-ceramics, which are bioactive and capable of forming a direct bond with bone, are usually brittle and have low fracture toughness and low resistance to impact loading, making them very limited in their use as load-bearing implants. Commercial dental and orthopedic implants coated with plasma-sprayed hydroxyapatite (HA) were developed to combine the superior mechanical properties of the metal together with the bioactivity and osteoconductivity of the Ca-P compounds. Typically, plasma-sprayed coatings consist of a mixture of amorphous and crystalline phases, and the amorphous and some of crystalline products such as tricalium phosphate (TCP) dissolve very fast while implanted in the human body.[7] Further heat treatment to improve crystallinity often results in cracking and loss of adhesion. To overcome these difficulties, many studies especially simple chemical treatment have been conducted in recent years. For example, bioactive titanium could be prepared by using NaOH or H_2O_2 (alone or a mixture of H_2O_2/HCl or H_2O_2/$TaCl_5$ solutions).[8–12] However, sodium titanate (by NaOH) thus formed had a high crack density and delaminated extensively from the Ti substrate, and crack-free titania with high bioactivity (by H_2O_2/$TaCl_5$) can be obtained only after being treated for a long time (80 °C, 72 h).[12,13] Therefore, improved synthetic routes to produce bioactive titanium are still required.

Nanostructured metals exhibiting unique physical, chemical, and mechanical properties have attracted tremendous attention to identify and exploit the unique properties and the new applications of these novel materials.[14] However, bulk nanostructured materials usually have very high strength but disappointingly low ductility producing insuperable problems for advanced structural applications.[15,16] The newly developed surface mechanical attrition treatment (SMAT), which introduces a large amount of defects and/or interfaces into the surface layer over a short period of time, is an effective way to realize surface self-nanocrystallization on metallic materials surface, and the grain size increases gradually with no obvious interfaces from top-surface to matrix.[17,18] It is a very promising method to produce functionally gradient materials since the nanocrystalline layer is suitable for surface modification, while the coarse-grained (CG) matrix provides the ductility.

The typical synthesis procedure includes the following steps: a commercial pure Ti plate with average grain size of 30 μm was first treated in vacuum by a SMAT machine for 60 min. The SMAT setup has been described in detail elsewhere.[17,18] After being pickled with 1 M HCl and carefully washed, the plate was immersed into 8.8 M H_2O_2/0.1 M HCl at 80 °C for 15 min (oxidation). Then the plates were dried at 40 °C for 6 h and calcinated at 400 °C in air for 1 h. For comparison, a CG sample was also prepared according to the same procedure only in the absence of SMAT and the pickling procedure was just the same as in ref 9. Both the SMAT and CG samples (Note: the SMAT and CG samples denote the Ti plate treated by oxidation and calcination thereafter if without special illustration) were washed by distilled water, dried in air, and finally soaked in simulated body fluid (SBF) at 37 °C to investigate the bioactivity. SBF that has almost the same ion concentration as human blood plasma was prepared as described in the literature.[8] The samples were taken out after having been immersed for 1 day, 7 days, washed gently with distilled water, and dried in an oven at 40 °C. The morphologies and microstructure of the as-prepared sample surfaces were characterized by optical microscopy (Leica, MPS30), field-emission scanning electron microscopy (FESEM: Supra 35 LEφ), and transmission electron microscopy (TEM: JEOL-2010), respectively.

Figure 1a is the cross-sectional optical microstructure of the Ti subjected SMAT only. It is obvious that the treated surface layer is much darker than the matrix. The deformation layers can accordingly be subdivided into two regions: (1) the severe deformation layers in which the grain boundaries could not be identified; and (2) minor deformation layers. A typical bright field image on top-surface is presented in Figure 1b. It is characterized by wavy-like and irregular grains with a large number of dislocations, and the corresponding selected area electron diffraction (SAED) inserted suggests the existence of both large and low angle grain boundaries. The average grain size was about 30 nm. Further investigations showed that a nanocrystalline layer of Ti with thickness about 30 μm was formed by SMAT, below which the grain size increased gradually.

* Corresponding author. Tel: +8621-34203743. Fax: +8621-34203742. E-mail: Gujf@sjtu.edu.cn.
[†] Shanghai Jiao Tong University.
[‡] Chinese Academy of Sciences.
[#] The Hong Kong Polytechnic University.

10.1021/cg070428a CCC: $37.00
Published on Web 12/05/2007

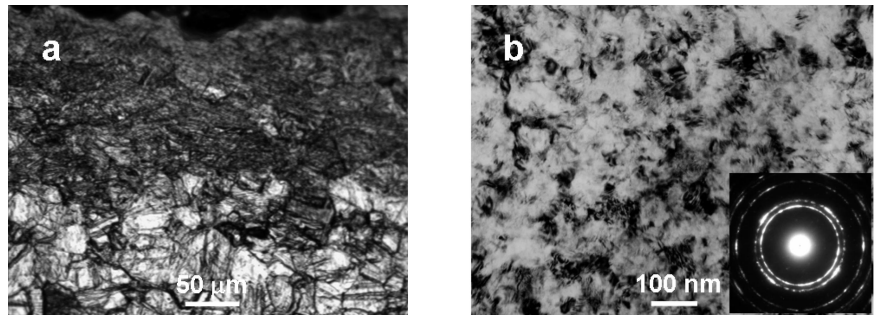

Figure 1. The microstructure of Ti subjected to SMAT only. (a) Cross-sectional optical micrograph; (b) Bright-field image of nanocrystalline Ti on top surface. Inset: corresponding SAED of (b).

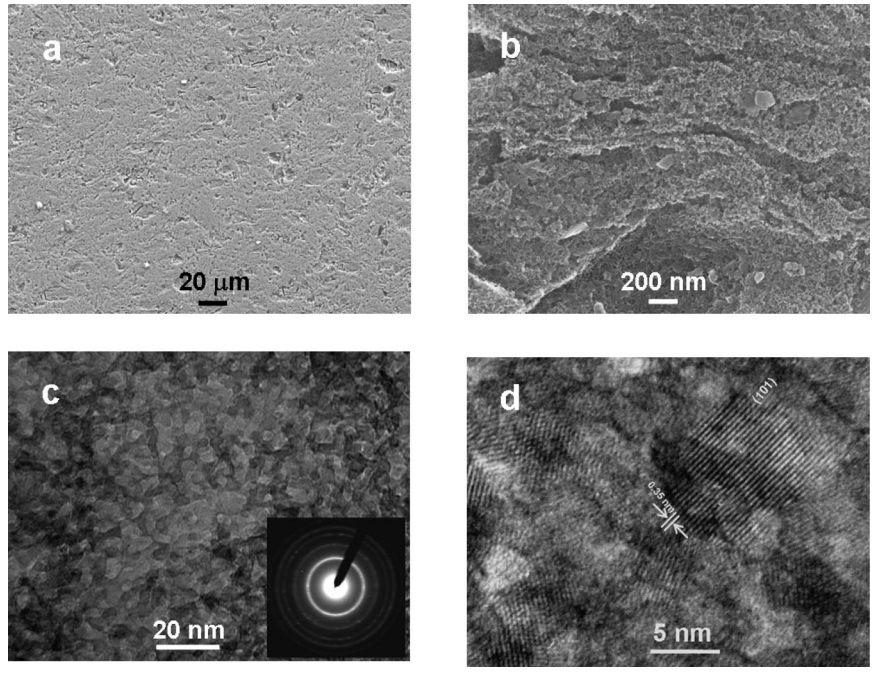

Figure 2. SEM (a, b) and TEM (c, d) images of SMAT Ti surface. Inset: corresponding SAED of (c).

After oxidation of the sample at 80 °C for 15 min and calcination at 400 °C for 1 h, no cracks existed in the SMAT sample surface (Figure 2a). Higher magnification displays that the surface is besprinkled with very small pores at the nanometer scale (Figure 2b). The porosity was further investigated by TEM. A perfect mesoporous structure with a pore size about 6 nm is formed in the SMAT sample (Figure 2c), and the corresponding SAED shows uniform rings of anatase. The grain size of anatase is about 10 nm with the {101} plane as presented in the high resolution TEM (HRTEM) picture (Figure 2d). The pore uniformity and the crystallinity are much more improved than the sample with the same treatment at room temperature.[19]

After the sample was soaked in the SBF for 1 day, a few isolated villous spherulites (1−2 μm) were generated on the SMAT Ti surface (Figure 3a), and a higher magnification inset shows they form directly on mesoporous anatase. The spherulite was further examined by TEM (Figure 3b). Spherulite is composed by numerous needle-like products tangling with each other, and the SAED inset shows clearly a ring of HA (211). After 7 days, numerous spherulites (8−10 μm) almost cover the whole surface (Figure 3c). The needle-like morphologies shows little change compared with 1 day, while the SAED is much more distinct, suggesting the improvement of the crystallinity (Figure 3d). The XRD results (not shown here) of the samples after being immersed in SBF for 7 days show that there is no crystalline bone-like apatite peak of the CG Ti, while there are two new peaks located at about 26° and 31.9° in the SMAT sample, respectively, corresponding well to the (002) and (211) of apatite.

As we mentioned before, CG Ti only formed sub-micrometer porous-like titania while being immersed in the H_2O_2 solution at 80 °C for sufficient time (20−30 min).[10] MacDonald et al. found that average grain size of nanocrystalline Ti film affects both oxidation kinetics and pore size of the titanium oxide layer while being immersed in H_2O_2, although they did not obtain mesoporous titania.[20−22] So it is very interesting to find that the nanocrystalline Ti can transform into mesoporous anatase by the present treatment. After SMAT, dense defects such as dislocations, vacancies, and a large volume fraction of grain boundaries with a high excess of stored energy were formed in the nanocrystalline Ti layer. The decomposition of H_2O_2 generating oxygen molecules and the diffusion of oxygen occur first at grain boundaries and grain interior with high defects density. Thus the titania formed operates in two ways: (1) the dissolution of titania by H_2O_2. It follows a reaction that produces surface-stabilized superoxide and peroxo anions as well as $Ti^{IV}(OH)_2$ species,[23] and a very small pit is left in situ on the surface; (2) the catalytic decomposition of H_2O_2 to H_2O and O_2.[24] Thereby the "new" titania undergoes the same process in successive cycles, and more pits are left in situ and aggregate with each other simultaneously. Finally, a perfect mesoporous structure comes into being just like the "electron avalanche" procedure. However, interactions between Ti and hydrogen peroxide are quite complicated, and further investigations are still necessary to clarify

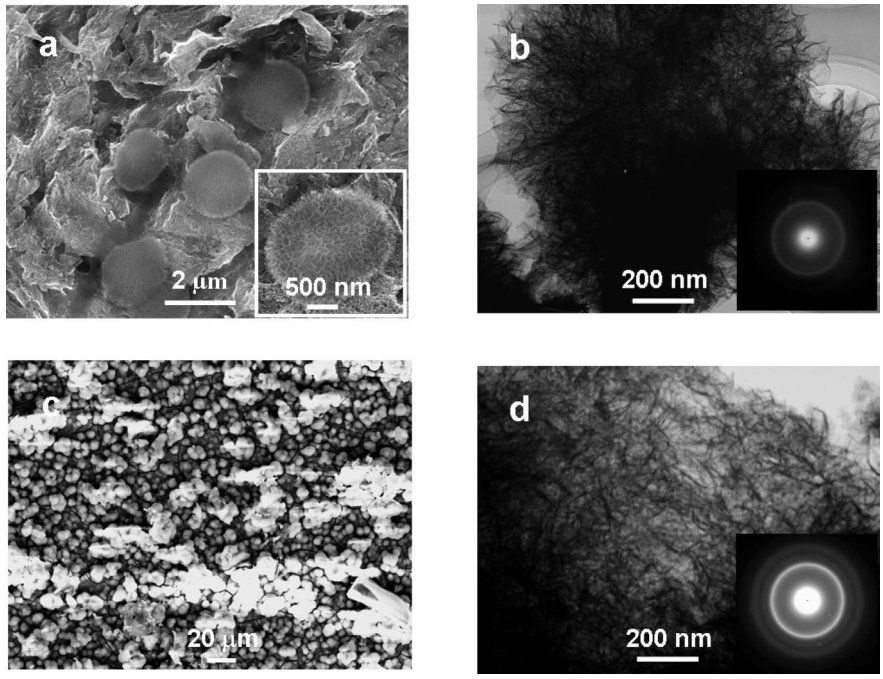

Figure 3. SEM and TEM images of HA on SMAT Ti surface: (a, b): HA for 1 day, the higher magnification of (a) is inserted in (a), the corresponding SAED of (b) is inserted in (b); (c, d): HA for 7 days. Inset: corresponding SAED of (d).

the formation mechanism of mesoporous structure. In the same time, the nucleation, the growth rates, and crystallinization capability of titania in the nanostructured surface are also greatly improved. The same procedure have been found in the nitriding and chromizing procedure at low temperature.[25–27]

The quick formation of HA particles on SMAT sample can be attributed to the unique nanostructured anatase on the SMAT sample surface, including the Ti-OH groups, negative surface charge, and the mesoporous structure. The anatase usually hydroxylates after being soaked in SBF, resulting in the formation of Ti-OH groups. It has been suggested that Ti-OH groups with a specific structural arrangement based on the anatase structure is effective in inducing apatite nucleation.[28,29] Furthermore, it can be inferred that the SMAT sample surface is negatively charged while being immersed in SBF with a pH value of 7.4 since the point of zero charge (PZC) of anatase (the pH value at which the surface charge of oxide is zero) is about 5.9,[30] which can lead to the establishment of an electrical double layer with an increased concentration of cations at the SMAT sample surface. Inside the mesopore, the superposition of the surface potential increases the ionic activity and thus increases the ionic concentrations, so the heterogeneous nucleation (apatite) is more likely to occur inside the pore.[31] Once the apatite nuclei form, they grow up and propagate spontaneously by consuming calcium and phosphate ions from the surrounding SBF and finally cover the whole surface. At the same time, the crystallinity of titania is also very important since it is well-known that amorphous titania has no bioactivity and it has been testified in refs 11, 13, and 32. Considering the relatively weak crystallinity of titania on present CG and SMAT samples treated at room temperature, it is reasonable that they show poor bioactivity while being immersed in SBF.

In conclusion, nanocrystalline Ti (~30 nm) was produced on bulk Ti by the SMAT method, and it further transformed into crack-free mesoporous anatase (~6 nm) by a simple chemical treatment. The mesoporous anatase shows high bioactivity while being soaked in SBF. To the best of our knowledge, it is the first report to produce bioactive mesoporous titania on bulk Ti by in situ synthesis without introducing external media (such as template, sputtering, or sol–gel methods). The hybrid SMAT method harmoniously combines chemical and mechanical treatment, and it is readily scaled up, opening a new area in the synthesis and application of titania. It gives new alternative approaches to functionally gradient materials by means of a nanostructure-selective reaction due to the much enhanced atomic diffusivity and chemical reactivity of the nanostructured surface layer.

Acknowledgment. This work was supported by NSFC (Grant No. 50431010), MOST of China (Grant No. 2005CB623604), and the Hong Kong Polytechnic University funds for niche areas (Grant No. BB90).

Supporting Information Available: XRD results of SMAT and CG samples after being immersed in SBF for 7 days. This material is available free of charge via the Internet at http://pubs.acs.org.

References

(1) Hench, L. L. J. *Am. Ceram. Soc.* **1998**, *81*, 1705–1728.
(2) Kokubo, T.; Kim, H. M.; Kawashita, M.; Nakamura, T. J. *Mater. Sci.: Mater. Med.* **2004**, *15*, 99–107.
(3) Long, M.; Rack, H. J. *Biomaterials* **1998**, *19*, 1621–1639.
(4) Liu, X. Y.; Chu, P. K.; Ding, C. X. *Mater. Sci. Eng. R* **2004**, *47*, 49–121.
(5) Thull, R.; Grant, D. in *Titanium in medicine*; Brunette, D. M., Tengvall, P., Textor, M., Thomsen, P., Eds.; Springer-Verlag: NY, 2001; Chapter 10, pp 287–334.
(6) Legeros, R. Z.; Craig, R. G. J. *Bone Miner. Res.* **1993**, *8*, S583–s596.
(7) Radin, S. R.; Ducheyne, P. J. *J Mater Sci: Mater. Med.* **1992**, *3*, 33–42.
(8) Kokubo, T.; Miyaji, F.; Kim, H. M. J. *Am. Ceram. Soc.* **1996**, *79*, 1127–1129.
(9) Wu, J. M.; Hayakawa, S.; Tsuru, K.; Osaka, A. *Scr. Mater.* **2002**, *46*, 705–709.
(10) Wang, X. X.; Hayakawa, S.; Tsuru, K.; Osaka, A. *Biomaterials* **2002**, *23*, 1353–1357.
(11) Wang, X. X.; Hayakawa, S.; Tsuru, K.; Osaka, A. J. *Biomed. Mater. Res.* **2000**, *52*, 171–176.
(12) Wu, J. M.; Hayakawa, S.; Tsuru, K.; Osaka, A. *Cryst. Growth Des.* **2002**, *2*, 147–149.
(13) Wu, J. M.; Hayakawa, S.; Tsuru, K.; Osaka, A. J. *Am. Ceram. Soc.* **2004**, *87*, 1635–1642.
(14) Lu, L.; Sui, M. L.; Lu, K. *Science* **2000**, *287*, 1463–1466.
(15) Koch, C. C.; Morris, D. G.; Lu, K.; Inoue, A. *Mater. Res. Soc. Bull.* **1999**, *24*, 54–58.
(16) Koch, C. C. *Scr. Mater.* **2003**, *49*, 657–662.

(17) Lu, K.; Lu, J. J. *Mater. Sci. Technol.* **1999**, *15*, 193–197.
(18) Lu, K.; Lu, J. *Mater. Sci. Eng.* **2004**, *A375*, 38–45.
(19) Wen, M.; Gu, J. F.; Liu, G.; Wang, Z. B.; Lu, J. *Surf. Coat. Technol.* **2007**, *201*, 6285–6289.
(20) Derosa, D. M.; Zuruzi, A. S.; Macdonald, N. C. *Adv. Eng. Mater.* **2006**, *8*, 77–80.
(21) Zuruzi, A. S.; Macdonald, N. C. *Adv. Fuct. Mater.* **2005**, *15*, 396–402.
(22) Zuruzi, A. S.; Kolmakov, A.; Macdonald, N. C.; Moskovits, M. *Appl. Phys. Lett.* **2006**, *88*, 102904.
(23) Murphy, D. M.; Griffiths, E. W.; Rowlands, C. C.; Hancock, F. E.; Giamello, E. *Chem. Commun.* **1997**, 2177–2178.
(24) Tengvall, P.; Lundstrom, I.; Sjoqvist, L.; Elwing, H. *Biomaterials* **1989**, *10*, 166–175.
(25) Tong, W. P.; Tao, N. R.; Wang, Z. B.; Lu, J.; Lu, K. *Science* **2003**, *299*, 686–688.
(26) Gu, J. F.; Bei, D. H.; Pan, J. S.; Lu, J.; Lu, K. *Mater. lett.* **2002**, *55*, 340–343.
(27) Wang, Z. B.; Tao, N. R.; Tong, W. P.; Lu, J.; Lu, K. *Acta. Mater.* **2003**, *51*, 4319–4329.
(28) Uchida, M.; Kim, H. M.; Kokubo, T.; Nakamura, T. J. *Am. Ceram. Soc.* **2001**, *84*, 2969–2974.
(29) Uchida, M.; Kim, H. M.; Kokubo, T.; Fujibayashi, S.; Nakamura, T. J. *Biomed. Mater. Res.* **2002**, *63A*, 522–530.
(30) Kosmulski, M. *Adv. Colloid interfac.* **2002**, *99*, 255–264.
(31) Pereira, M. M.; Hench, L. L. J. *sol-gel sci. technol.* **1996**, *7*, 59–68.
(32) Uchida, M.; Kim, H. M.; Kokubo, T.; Fujibayashi, S.; Nakamura, T. J. *Biomed. Mater. Res. A* **2002**, *64*, 164–170.

CG070428A